SUPPLEMENTARY FIGURES

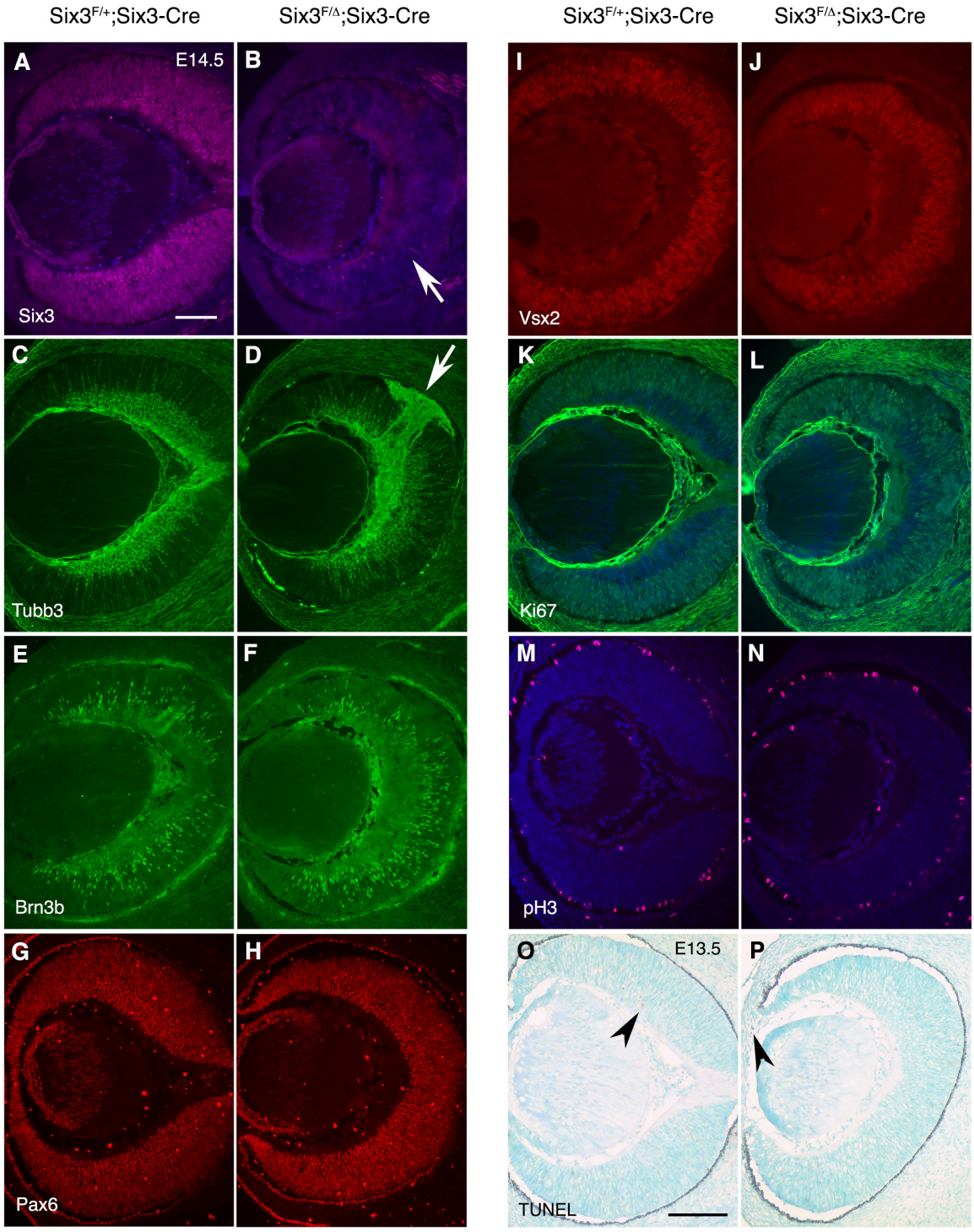

Fig. S1. Characterization of type I (morphological normal) *Six3*$^{Six3\text{-}Cre\ KO}$ retinae at E13.5-14.5. Related to Figs 2, 3. Panels A-N were at E14.5 and panels O-P were at E13.5. The results represent three morphologically normal mutant embryos. **(A, B)** Six3 was efficiently deleted in the NR (arrow in B). Mutant NR was slightly smaller. **(C, F)** Retinal ganglion cell differentiation was grossly unaffected, as indicated by normal

Tubb3 and Pou4f2 expression. Occasionally, axon pathfinding errors were found (arrow in D, n=1/3). **(G-J)** Retinal progenitors were grossly unaffected, as indicated by normal Pax6 and Vsx2 expression. **(K-N)** Ki67 and pH3 expression in the control and *Six3*$^{Six3\text{-}Cre\ KO}$ retinae at E14.5. pH3 index in type I *Six3*$^{Six3\text{-}Cre\ KO}$ mutant retinae at E14.5 was slightly reduced without statistic significance (6.77E-05 ± 6.45E-06 vs. 7.53E-05 ± 4.99E-06, *p*=0.259, *t*-test). The pH3 index was calculated as the ratio of the number of pH3-positive cells over the areas of retinal epithelium, assuming that the total number of retinal cells is proportional to the size of retinal epithelium in the control and type I Six3$^{Six3\text{-}Cre\ KO}$ mutant retinae. Two wild type and three *Six3*$^{Six3\text{-}Cre\ KO}$ mutant retinae at E14.5 were quantified using ImageJ. **(O-P)** TUNEL assay. Apoptosis was rarely found in both the control and type I *Six3*$^{Six3\text{-}Cre\ KO}$ retinae at E13.5. A few apoptotic cells indicated that TUNEL assay worked (arrowheads in O, P). Scale bars = 100 μm.

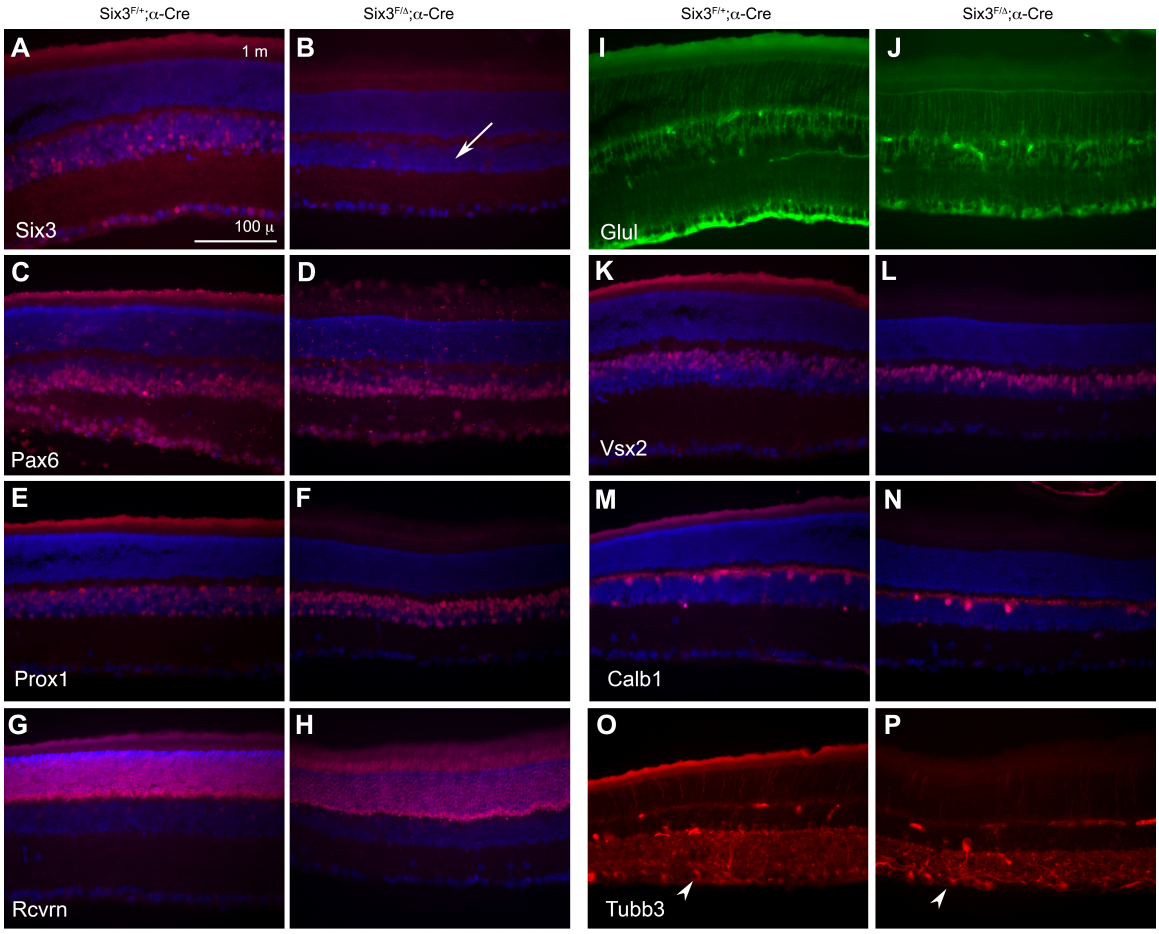

Fig. S2. Retinal cell fate determination is normal in Pax6 α-Cre mediated Six3-deficient retinae. Related to Figure 3. Represent three retinae. Six3 was conditionally deleted in distal retinae using Pax6 α-Cre. Distal regions of the control and Six3-deficient retinae at 1-month stage were used for immunostaining. (**A**, **B**) Six3 was efficiently deleted in distal regions. (**C**-**P**) Major retinal cell types were present in *Six3* mutant retinae, as indicated by a panel of markers. Scale bars, 100 μm.

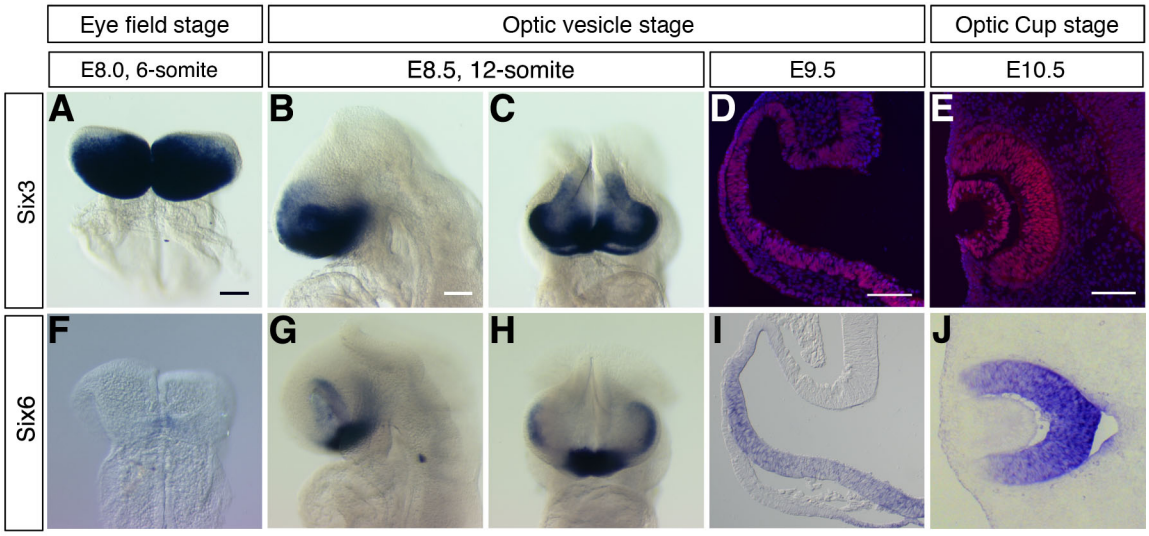

Fig. S3. Comparison of *Six3* and *Six6* expression during retinal development. Related to Figs 2, 4. The results represent three embryos at each stage. **(A-J)** In mouse retinal development, *Six3* expression (A) preceded *Six6* expression (F), and was localized in the anterior neural plate, including the eye field. At E8.5, *Six3* expression was strong in the evaginating optic vesicles (B, C), but *Six6* expression was still weak in optic vesicles (G, H). At E9.5 and E10.5, the expression of Six3 and that of *Six6* overlapped in the ventral optic vesicles (D, I) and the inner layer of optic cups (E, J). Scale bars, 100 μm.

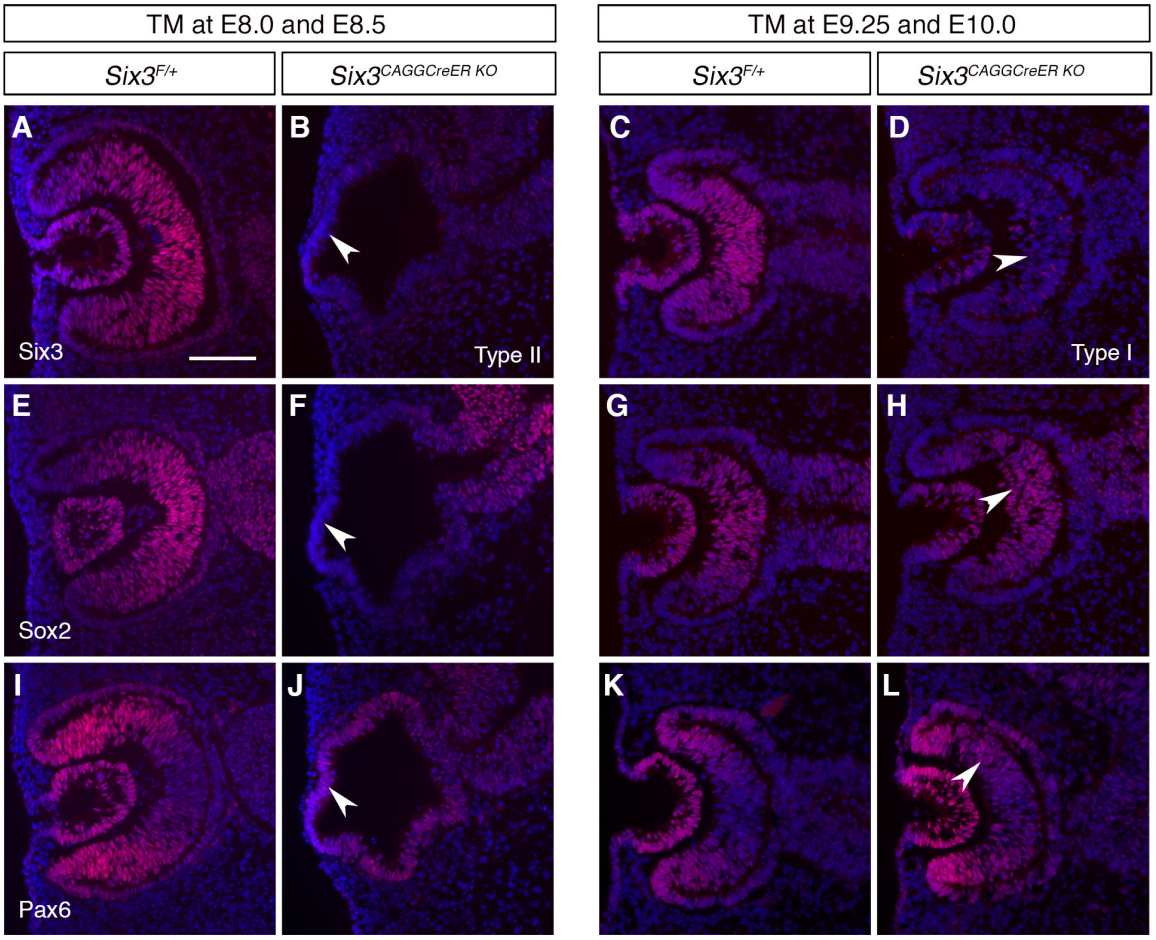

Fig. S4. Early (E8.0-8.5) and late (E9.25-10.0) *Six3*-deficiency causes type II and type I phenotypes, respectively. Related to Fig. 2. The results represent three out of three mutant embryos**.** *Six3* was temporally deleted using CAGG-CreER at early and late phases by administration of Tamoxifen (TM): two doses at E8.0 and E8.5 for early phase deletion, and two doses at E9.25 and E10.0 for late phase deletion. Embryos were harvested at E10.5 for molecular characterization. **(A-D)** Six3 was efficiently deleted at both phases (arrowheads in B, D). **(E-L)** Upon early deletion, *Six3*-deficient embryos displayed type II phenotypes: optic cups did not form, NR marker Sox2 was absent, and NR and RPE marker Pax6 was expressed in the whole defective vesicles (arrowheads in F, J). Upon late deletion, *Six3*-deficient embryos exhibited type I phenotypes: optic cups formed normally, and Sox2 and Pax6 were expressed normally compared with those in the controls (arrowheads in H, L). Scale bar = 100 μm.

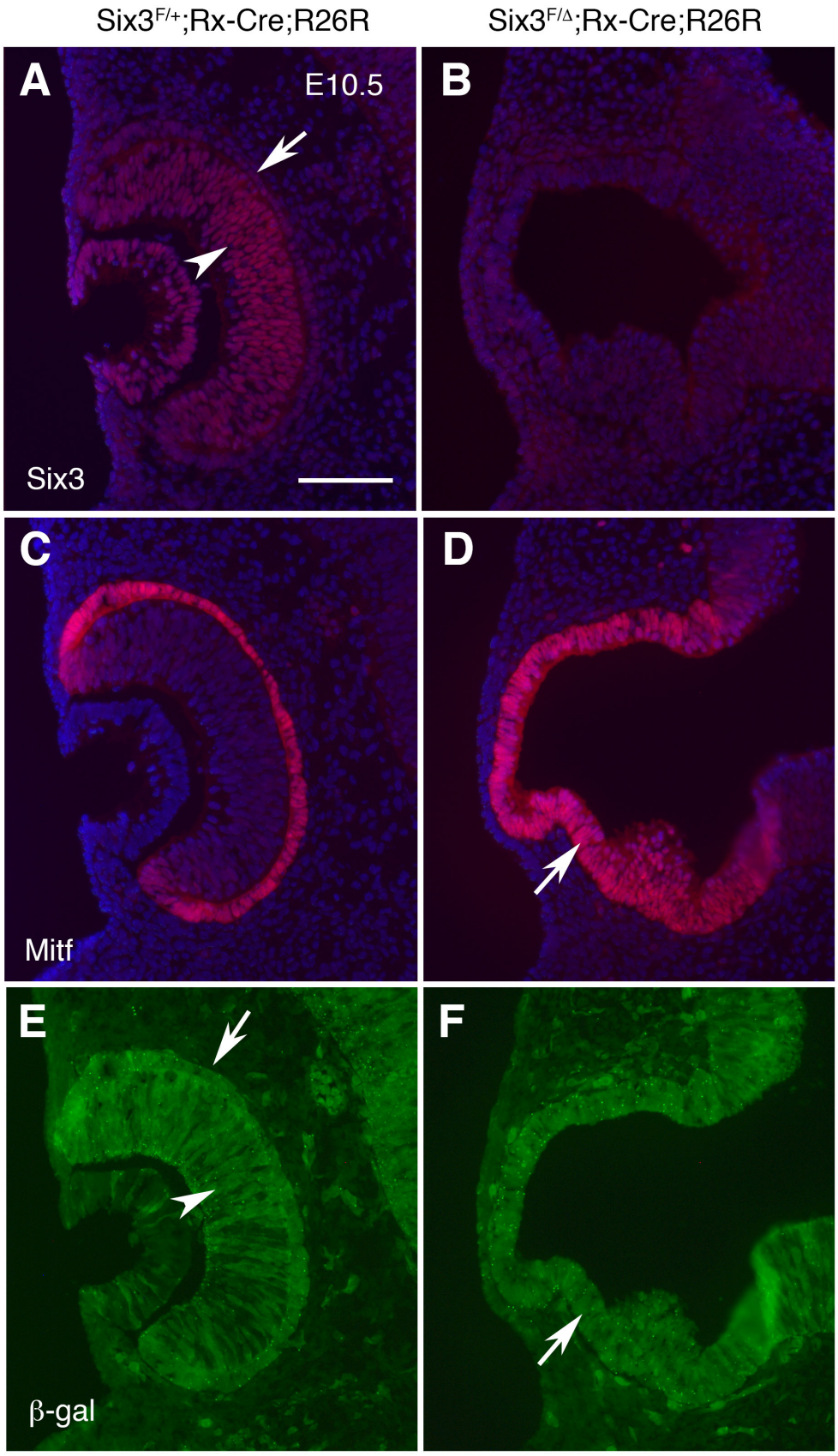
Six3F/+;Rx-Cre;R26R
Six3F/Δ;Rx-Cre;R26R
A
E10.5
B
Six3
C
D
Mitf
E
F
β-gal

Fig. S5. Gene expression in R26R locus is active in RPE cells and does not require Six3 functions. Related to Fig. 5. (**A**-**D**) At E10.5, Six3 was highly expressed in the NR but was significantly downregulated in the RPE (arrowhead and arrow in A). When Rx-Cre was used as a deleter, Six3-deficiency disrupted NR specification but did not affect RPE formation (A-D). (**E**, **F**) Rx-Cre positive progenies were found in both NR and RPE in E10.5 control embryos (arrowhead and arrow in E). Importantly, the remnant RPE in the $Six3^{Rx\text{-}Cre\ KO}$ mutant embryos expressed R26R reporter for Rx-Cre, indicating that gene expression in R26R locus is active in RPE and does not require Six3 functions (arrow in F). Scale bar, 100 μm.

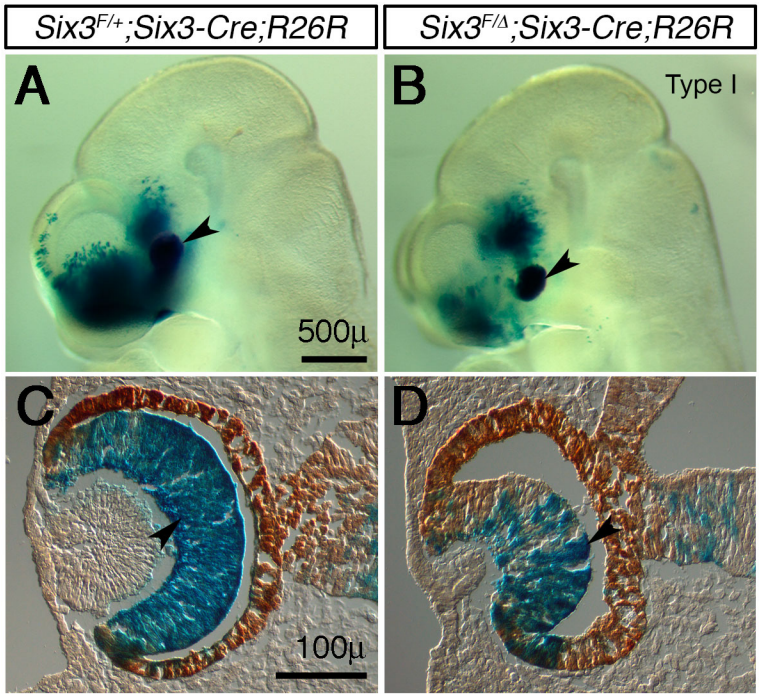

Fig. S6. Six3-Cre positive progenies remain in type I *Six3*$^{Six3\text{-}Cre\ KO}$ retinae. Related to Fig. 5. The results represent three mutant embryos. **(A-D)** Embryos from the breeding between female *Six3*$^{F/F}$*;R26R/R26R* mice and *male Six3*$^{+/\Delta}$*;Six3-Cre* mice were harvested at E10.5 for X-gal staining. Control and type I mutant embryos (defined by normal morphology in the eyes, n = 3) were sectioned and immunostained with a Mitf antibody. In type I *Six3*$^{Six3\text{-}Cre\ KO}$ embryos, optic cups formed, Mitf expression was grossly normal, and ß-gal positive cells remained in NR (arrowheads in A-D). Occasionally, type I optic cups were smaller than control optic cups (n=2/26). Scale bars, 500 µm (A) and 100 µm (C).

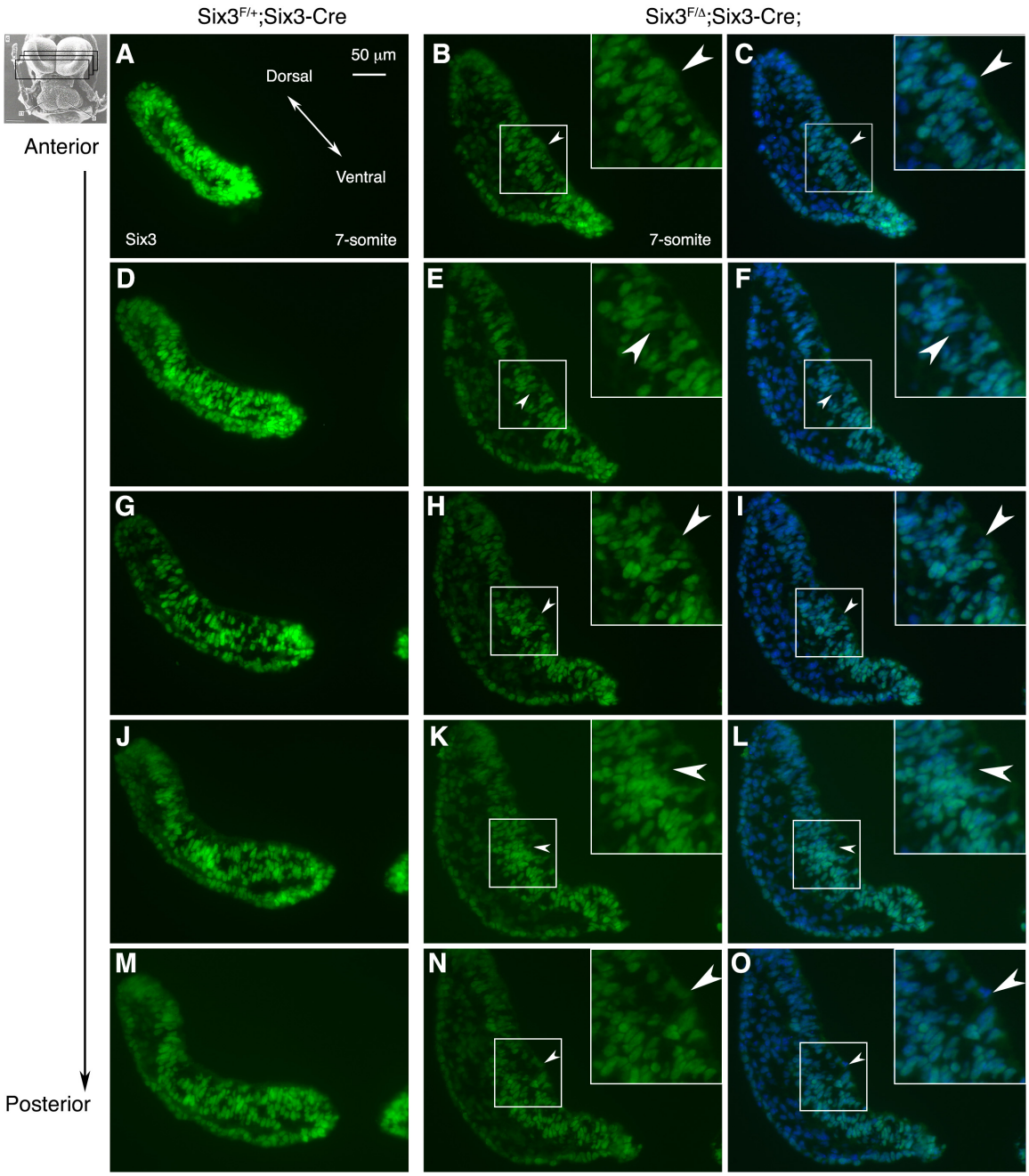

Fig. S7. Six3-deletion in 7-somite *Six3*$^{Six3\text{-}Cre\ KO}$ embryos. Related to Fig. 6. Serial coronal sections of 7-somite embryos were used for immunostaining. The images were processed the same way and thus the intensity of fluorescence reflects Six3 expression. (**A**-**O**) In the control embryos, Six3 expression displayed a gradient along anteroposterior axis and ventrodorsal axis, with high levels at the anteroventral eye field / optic pit (A,D,G,J,M). In *Six3*$^{Six3\text{-}Cre\ KO}$ embryos, Six3-deletion was found in a small population of progenitors (arrowheads in B,C,E,F,H,I,K,L,N,O), and the gross reduction of Six3 expression was striking at the anteroventral eye field / optic pit, consistent with the pattern of R26R reporter expression for Six3-Cre at 8- to 11-somite stages. Interestingly,

Six3-deficient cells appeared to be disintegrated from retinal epithelium (arrowheads in B,C,H,I,K,L,N,O), indicating that Six3-deficient cells were dying. Scale bar, 50 μm.

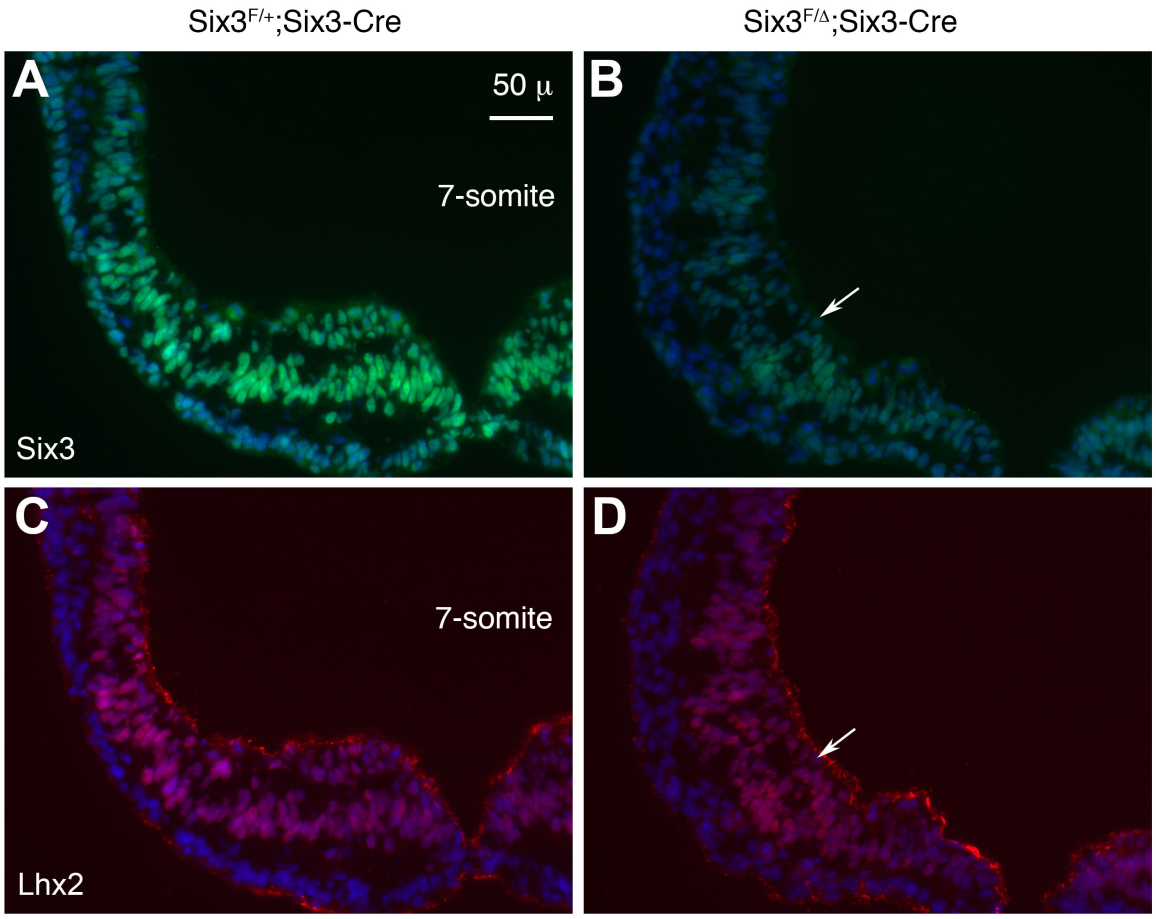

Fig. S8. Lhx2 expression is slightly reduced in Six3$^{Six3\text{-}Cre\ KO}$ mutant embryo at 7-somite stage. Related to Fig. 6. Immunostaining of Six3 and Lhx2 was performed. (**A**, **B**) Six3 was absent in a small population of retinal progenitors (arrow in B). Overall reduction of Six3 expression in Six3$^{Six3\text{-}Cre\ KO}$ mutant embryos was caused by germline Six3-deletion in one *Six3* allele (A, B). (**C**, **D**) Lhx2 expression was slightly reduced in Six3$^{Six3\text{-}Cre\ KO}$ mutant retinal progenitors (arrow in D). Scale bar, 50 μm.

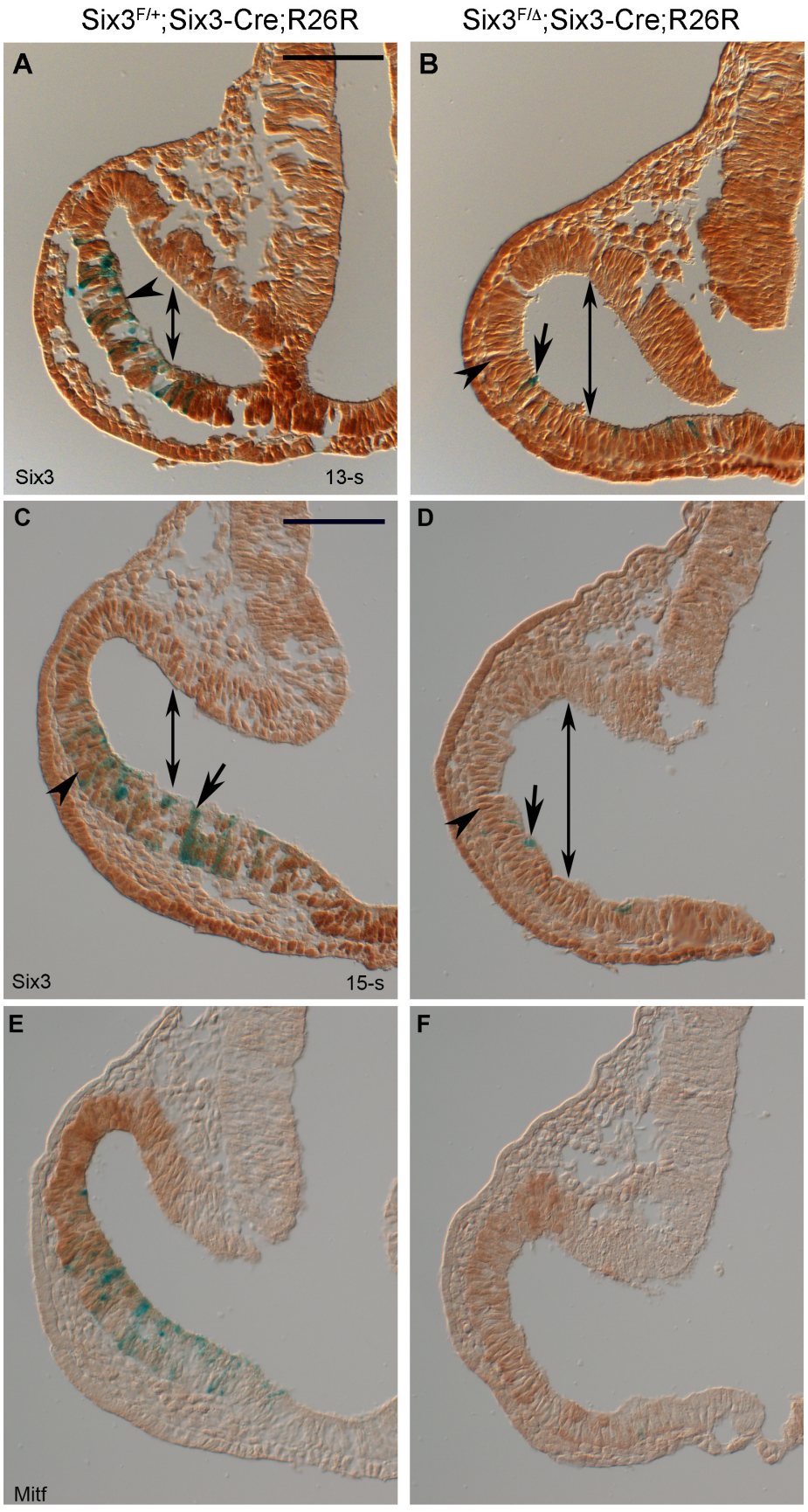
Six3F/+;Six3-Cre;R26R
Six3F/Δ;Six3-Cre;R26R
A
B
Six3
13-s
C
D
Six3
15-s
E
F
Mitf

Fig. S9. Six3-deletion and R26R reporter expression in Six3$^{Six3\text{-}Cre\ KO}$ mutant embryos. Related to Fig. 6. (**A**-**F**) Morphological defects were obvious (double-headed arrows in A-D). At 13-somite stage, the number of β-gal positive cells was drastically reduced in the mutant embryos, and the remaining β-gal positive cells were clearly negative for Six3 and appeared to be disintegrated from retinal epithelium, indicating that the Six3-deficient cell was dying (arrow in B). In the β-gal negative cells, Six3 immunostaining remained (arrowheads in A, B). Similar results were found in mutant embryos at 15-somite stage (C, D). In addition, Mitf expression was expanded in 15-somite mutant embryo (E, F). Scale bars, 100 μm.

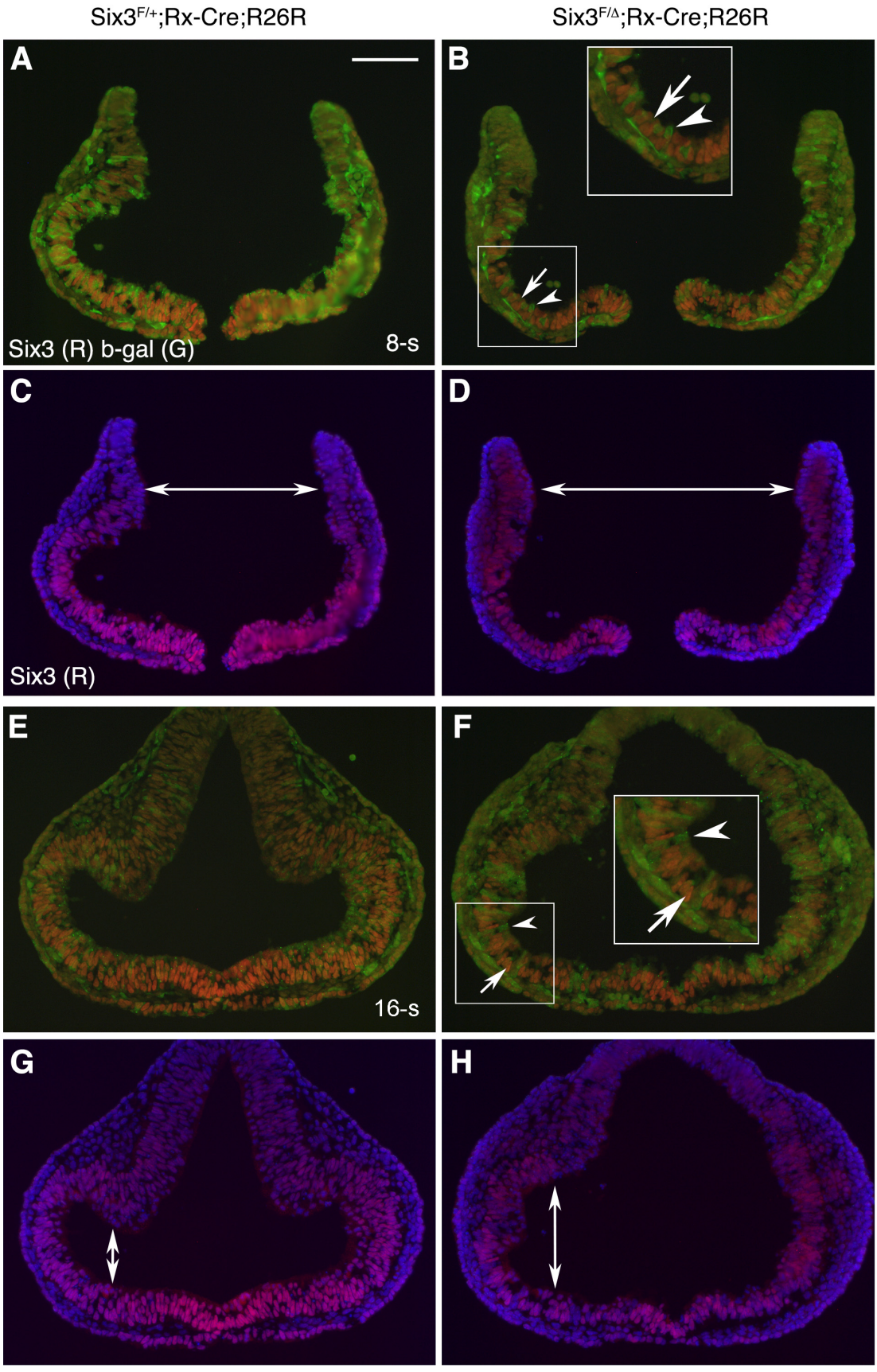
Six3F/+;Rx-Cre;R26R
Six3F/Δ;Rx-Cre;R26R
A
B
Six3 (R) b-gal (G)
8-s
C
D
Six3 (R)
E
F
16-s
G
H

Fig. S10. Six3-deletion and R26R reporter expression in Six3$^{Rx\text{-}Cre\ KO}$ mutant embryos driven by Rx-Cre. Related to Fig. 6. (**A**-**H**) In the control embryos at 8-somtie stage, R26R reporter for Rx-Cre was widely expressed (A). In Six3$^{Rx\text{-}Cre\ KO}$ mutant embryos driven by Rx-Cre, however, the number of R26R reporter positive cells was reduced (B). Accordingly, Six3 was only partially deleted (B, D), and Six3-positive cells and β-gal positive cells were mutually exclusive. Despite partial Six3-deletion, drastic morphological changes were observed (double-headed arrow in C, D). Similar results were found in 16-somite Six3$^{Rx\text{-}Cre\ KO}$ mutant embryos (E-H). Scale bar, 100 μm.

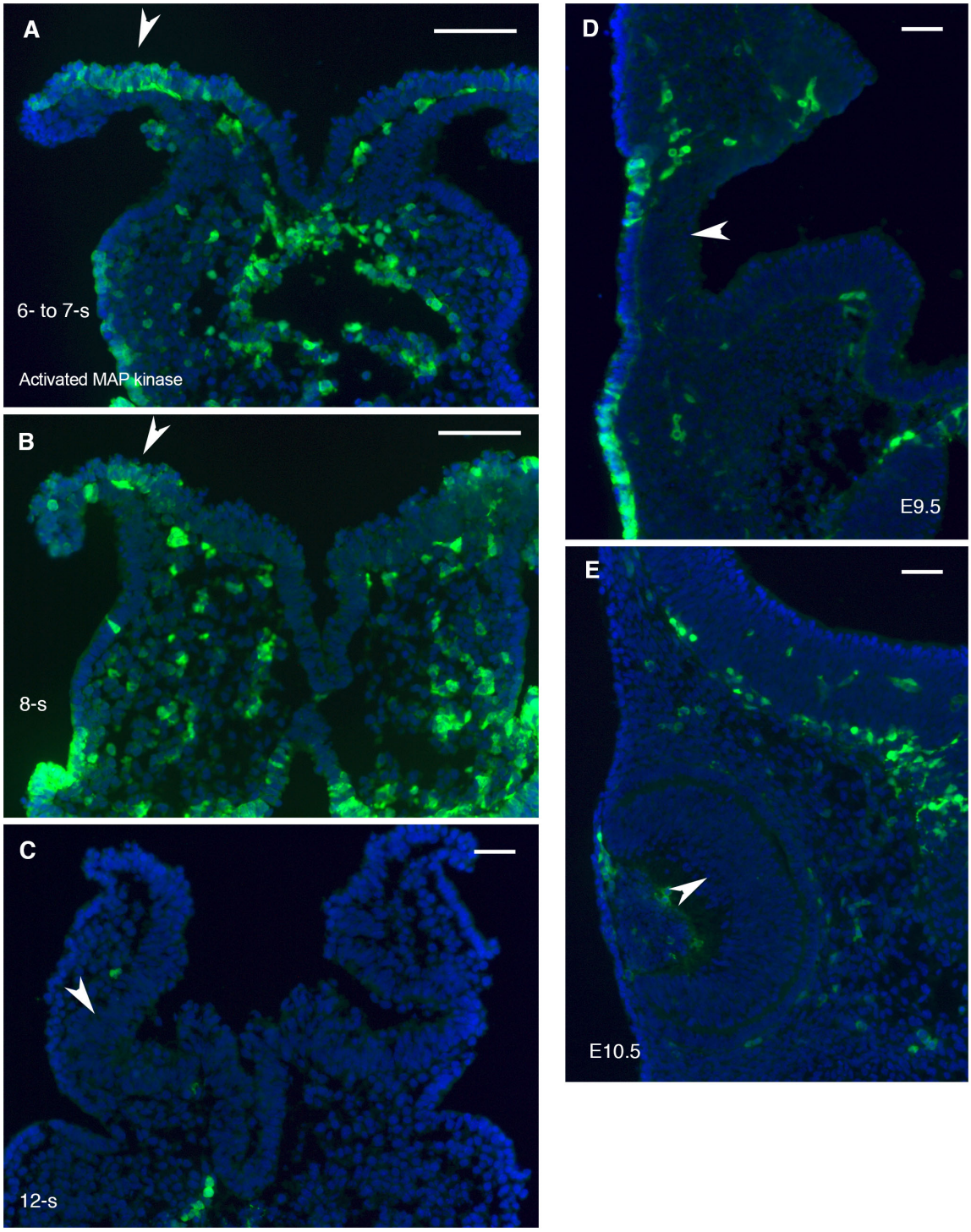

Fig. S11. Activated MAP kinase/dpERK-1&2 signaling is found in early retinal development. Related to Fig. 6. The results represent two embryos at each stage. **(A-E)** Activated MAP kinase was found in some cells in the optic pits at 6- to 8-somite stages (arrowheads in A-B), but was downregulated at later stages during retinal development (arrowheads in C-E). Scale bars, 100 μm.

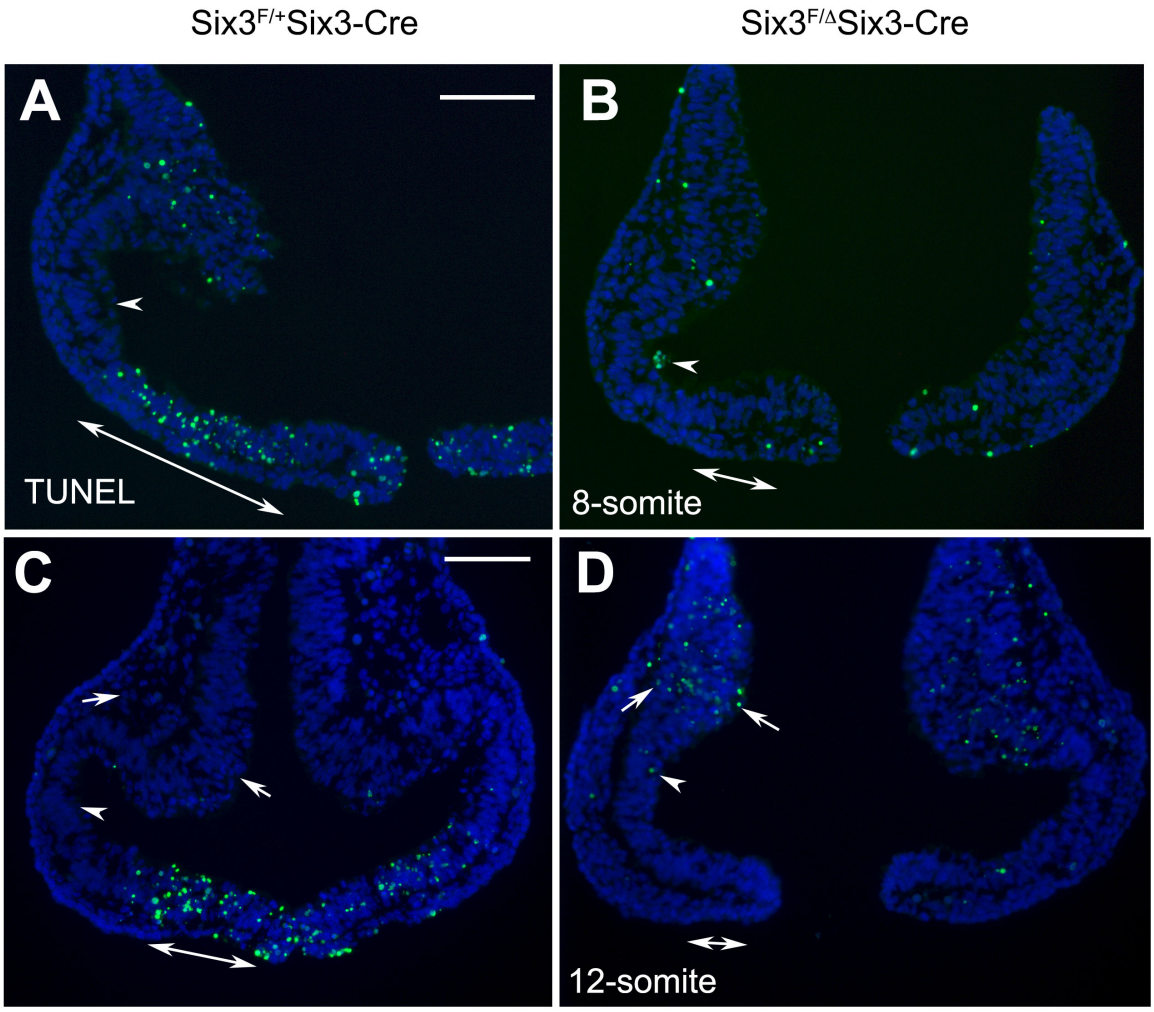

Fig. S12. Apoptosis profiles in *Six3*$^{Six3\text{-}Cre\ KO}$ embryos at 8- and 12-somite stages. Related to Fig. 6. Represent three embryos. (**A-D**) Ectopic apoptosis at the optic pits/vesicles was found at 8-somite stage but became rare at 12-somite stage (arrowheads in A-D). Ectopic apoptosis in the dorsal optic vesicles and the dorsal periocular mesenchyme were observed at 12-somite stage (arrows in C, D). Physiological apoptosis at the ventral optic stalks and anteroventral neural ridge was significantly reduced (double-headed arrows in A-D). In addition, anterior neuropore closure was delayed in *Six3*$^{Six3\text{-}Cre\ KO}$ mutant embryos (C, D). Scale bars, 100 μm.

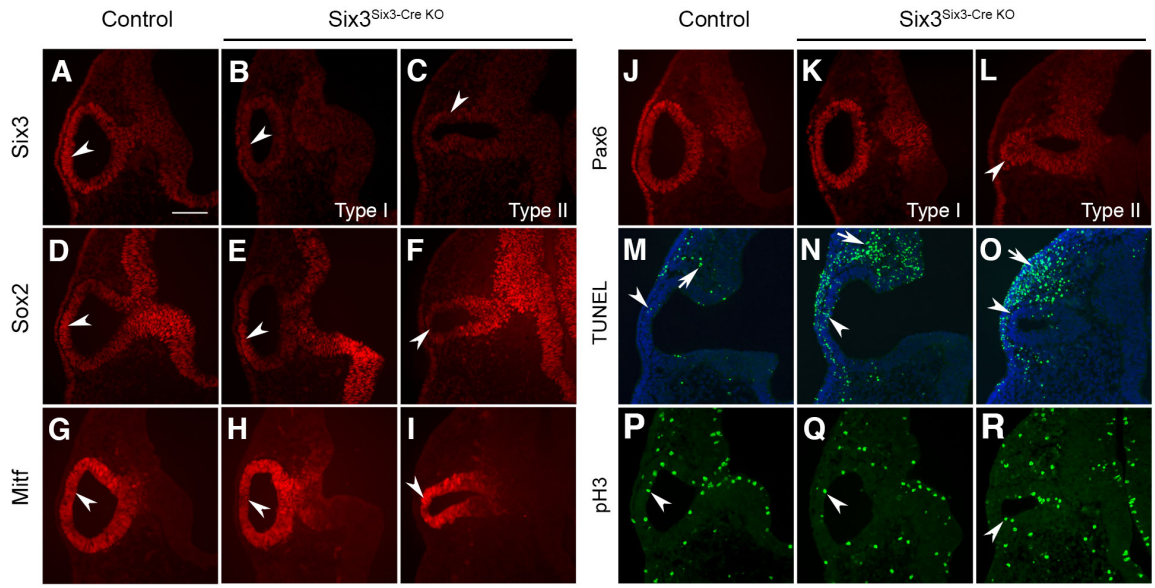

Fig. S13. Characterization of *Six3*$^{Six3\text{-}Cre\ KO}$ embryos at E9.5. Related to Figs 2, 6. The results represent three mutant embryos. Transverse sections at E9.5 were used for immunostaining. **(A-C)** Six3 expression was downregulated in both type I and II *Six3*$^{Six3\text{-}Cre\ KO}$ embryos. In type II *Six3*$^{Six3\text{-}Cre\ KO}$ embryos, the morphology of optic vesicles was defective (arrowheads in A-C). **(D-F)** In the control and type I *Six3*$^{Six3\text{-}Cre\ KO}$ embryos, NR marker Sox2 became restricted to the prospective NR territory in the optic vesicle (arrowheads in D, E). In type II *Six3*$^{Six3\text{-}Cre\ KO}$ embryos, the prospective NR is missing, as indicated by the lack of Sox2 expression (arrowhead in F). **(G-H)** RPE marker Mitf started to became downregulated in the prospective NR in the control and type I *Six3*$^{Six3\text{-}Cre\ KO}$ optic vesicles, but Mitf was continuously strong in type II *Six3*$^{Six3\text{-}Cre\ KO}$ defective vesicles (arrowheads in G-I). **(J-L)** Levels of Pax6 expression were comparable in the control and *Six3*$^{Six3\text{-}Cre\ KO}$ embryos (arrowhead in L). **(M-O)** Compared with that in the controls, apoptosis was grossly normal in the mutant optic vesicles, but was substantially increased in the periocular mesenchyme (arrowheads and arrows in M-O, respectively). **(P-R)** pH3 expression in the control, type I and type II *Six3*$^{Six3\text{-}Cre\ KO}$ embryos (arrowheads in P-R). Scale bar, 100 μm.